GI_Forum 2023, Issue 2
Page: 69 - 87
Full Paper
Corresponding Author:
jan-peter.mund@hnee.de
DOI: 10.1553/giscience2023_02_s69

Remote Sensing Methods Combined with Anti-collision Systems to Reduce Avian Collisions with Wind Turbines, Facilitating the Energy Transition

Jan-Peter Mund[1] and Siegfried Rieger[1]
[1]Hochschule für Nachhaltige Entwicklung, Eberswalde, Germany

Abstract

In the transition to renewable energies, the presence of large birds and birds of prey leads to conflicts of interest between nature conservation and achieving energy targets, especially in the construction of wind farms. The birds at risk of collision with wind turbines are frequently protected species, which presents a barrier to gaining approval of suitable areas and to the actual siting of new wind farms. The implementation of innovative anti-collision systems, particularly AI-supported radar or stereoscopic camera systems, could reduce the risk of bird collisions with wind turbines. We present an independently controlled empirical study examining the bird detection rate and species classification accuracy of two technically different remote-sensing sensor types: a stereo-camera system and a radar scanning system. The results support the hypothesis that modern anti-collision systems have the potential to detect, recognize, track and correctly classify bird species. They further underline that anti-collision systems can be effective in reducing avian collisions with turbine blades, particularly if the all-weather radar's multi-object, close to 360° scanning capability is combined with the high accuracy of AI-based image recognition from stereo-camera systems.

Keywords:

anti-collision system, stereo camera, bird scanning radar, wind turbines, renewable energy transformation

1 Introduction, problem statement and research statement

The transition to renewable energy, particularly wind energy, is essential to tackle climate change and protect biodiversity, but the expansion of wind farms is hampered by conflicts with species conservation (KNE, 2020a). Advances in technology and engineering are leading to denser wind farms (Gradolewski et al., 2021). The higher engine positions and longer blades of modern wind turbines pose a significant risk of injury or death to bird populations from collision, further increasing opposition to wind turbines due to their impact on birds and bats in particular (Davy et al., 2021).

The presence of large birds and birds of prey, which are often protected species, fuels administrative conflicts in the legal approval and designation of suitable areas and the actual siting of new wind farms (Figure 1) (Fachgruppe Rotmilan der Deutschen Ornithologen-Gesellschaft, 2022; Lag Vsw, 2015). Birds of prey such as the Red Kite or the White-tailed Eagle are endangered globally, and are listed among the avian species most affected by collisions with wind turbines. Data from the NGO NABU show a downward trend in the Red Kite population in Germany over the entire period 1988 to 2014. In the period 2000 to 2015, 4.5% of all Red Kite deaths were caused by collisions with wind turbines, and the proportion of all bird and bat deaths from the same cause increased more than fourfold, from 2% to 9% (for further detailed data, see NABU Facts Check Red Kite, 2016).

The Red Kite (*Milvus milvus*), which is endangered in Europe, has its main distribution area in Germany. More than half of the world's population breeds here. A medium-sized bird of prey, its body length varies between 60 and 73 centimetres; its tail is between 31 and 39 centimetres long; its wingspan measures between 150 and 180 centimetres. Distinctive features are a slender silhouette with long wings, narrow wings in flight, a deeply forked tail, and its rusty ground colour (NABU, 2016).

The White-tailed Eagle (*Haliaeetus albicilla*) is a bird of prey that lives in Eurasian aquatic landscapes from Greenland to the Pacific Ocean. They are among the largest birds of prey in Europe, reaching a length of 74 to 92 centimetres and a wingspan of 193 to 244 centimetres. The species is easily identified: they have a long, powerful neck, and broad, plank-shaped wings in addition to their large size and white tail (Krüger et al., 2010).

Many countries have regulations to protect wildlife from the negative impacts of wind farms. In Germany, the Federal Agency for Nature Conservation implements planning and operating guidelines (BfN et al., 2020) that include anti-collision systems (ACS) to minimize harm to birds and bats in wind farms. In many federal states, species-specific distance recommendations, known as animal-ecological distance criteria, are set as preventative measures to protect breeding sites of endangered bird species, due to which large areas, even far from settlements, are excluded as sites for wind farms (Georgiev et al. 2022). Other areas designated as suitable for wind farms are not fully exploited, partly because of the animal-ecological distance criteria (OVG Lüneburg, 2019). Anti-collision systems are, therefore, important in the development of wind energy projects, facilitating regulatory requirements and public acceptance (Langgemach & Dürr, 2021).

The use of ACS, particularly radar or stereoscopic camera systems, could reduce the risk of birds colliding with wind turbines (WT) (Albertani & Johnston, 2021). However, current knowledge of the performance, accuracy and site-suitability of typical ACS systems is limited (KNE, 2020a). The effectiveness of an ACS may vary depending on its specific design, the bird species present near the wind turbines, and the location of the turbines. Independent, controlled empirical tests of ACSs in characteristic landscapes are essential to improve scientific and administrative knowledge about their quality and success rate.

The objective of this study is to analyse the detection rate and classification accuracy of two different technical types of ACS in order, potentially, to reduce collisions with simulated wind turbines by sensitive species such as the Red Kite, White-tailed Eagle and other larger birds of prey. This empirical field study in characteristic landscapes provides insights into the capacity, effectiveness and accuracy of the two types of ACS for bird detection.

Figure 1: Red Kite close to WT (photo Mund, 2022)

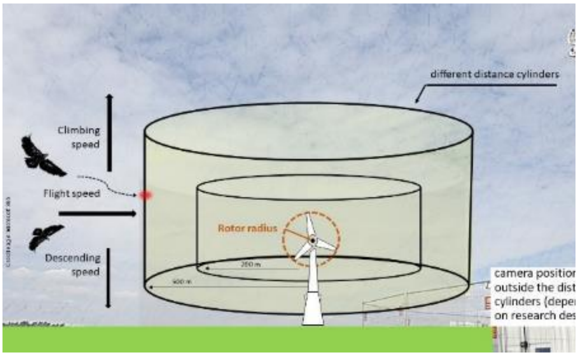

Figure 2: Anti-collision systems and distance criteria at WT (own graphic 2023)

2 Study locations, materials and method

A stereo-optical camera system and a radar system for the detection and classification of bird species were tested in 2022 at two test sites in Brandenburg. The design of the study followed a systematic technical protocol (see Kompetenzzentrum Naturschutz und Energiewende (KNE), 2019b)), and the test sites were selected based on criteria such as landscape variability, high diversity of bird species and high flight activity (Table 1). An advisory group of regional stakeholders from conservation authorities, NGOs and civil society reviewed all criteria and observed the applied research methodology. The sites was equipped with two different bird-detection AC systems – the e3's stereo-camera system 'mobile IdentiFlight', and the radar system 'BirdScan MS1' distributed by Swiss Birdradar Solution AG (Figure 4).

Table 1: Criteria for test-site selection derived from the structure of the landscape (left) and the occurrence of avifauna (right)

Structural landscape characteristics	**Occurrence of avifauna species for Brandenburg**
Higher topographic variation at the complex site	Spatial proximity to potential eyrie sites of target species
Small-scale structural units (numerous hedges, copses) at the complex site.	Relative proximity to diversely structured forest edges at both sites

Low relief energy at the open-land site	Above-average flight activity of the target species
Few structural units (hardly any hedges or woody plants) at the open-land site	Low numbers of migratory or resting birds at the site

The first test site is located to the north of the Peetzig Estate on a large area of arable land with a south-easterly slope. It is surrounded by mixed pine woodland and taller hedgerows to the north, with Peetzig village and Lake Peetzig to the south. In 2020, Red Kite nests were found in the mixed forest. White-tailed Eagle and buzzard nests were found south of Lake Peetzig. The ACS is located at UTM 33 N, ETRS 32633, with x = 426808.5, y = 5881390.0, at 72m above sea level. (See Figure 3 for the test site.)

Figure 3: Test site 1 – flat open agricultural landscape (photo Mund, 2022)

Figure 4: Test site 2 – complex undulating landscape (photo Mund, 2022)

The second test site (Figure 4), on a glacial hilltop surrounded by linear woodland and hedgerows, is located west-northwest of the Peetzig Estate. West of the site itself are large mixed coniferous and deciduous forests, where White-tailed Eagles nest. South of the summit are the Small Peetzig Lakes, where Red Kite nests were mapped in 2020. This second test site is categorized as 'complex'; the ACS is located at UTM 33 N, ETRS 32633, x = 426054.5, y = 5880728.0, at 82m above sea level.

We adapted the experimental ACS set-up proposed in KNE (2019a) to the local landscape conditions of the test sites, the ACSs selected, the empirical measurements required, and the statistical test of our chosen methodology. As there are no WTs installed at the test sites, virtual anti-collision cylinders were programmed around each virtual WT location to be monitored (Figure 2). We calculated the shutdown times for each WT in order to meet the legal requirements for the 'spin to trundle' operation (ENERCON, 2020). A pre-calculated, species- and system-specific distance cylinder automatically generates the shutdown signal after bird detection and classification. Such virtual cylinders, or “geofences”, are three-dimensional spaces in which the target bird species can trigger an anti-collision signal. The specific values were calculated individually for each test site, depending on the landscape structure, the targeted WT, bird species and the type of ACS installed (Figure 2).

The calculation of the species-specific virtual distance cylinders (Figure 2) is based on the medians of the horizontal flight speed, the descent rate, the climb rate, and the shutdown time of the WT (Aschwanden & Leichti, 2020; Bruderer & Boldt, 2001). The formulae for all site-specific calculations were taken from a report on ACS published by ARSU GmbH in 2021. The hysteresis (= delay between individual shutdown signals) was set to 3 minutes for both types of ACS. Table 2 shows the species-specific virtual distance cylinder parameters.

Table 2: Parameters of species-specific virtual cylinders: distances to WT

Distance to WT cylinder determination	**Red Kite**	**White-tailed Sea Eagle**
Distance cylinder radius	372.5m	502m
Distance cylinders for the stereo-camera system - **Lower limit**	70m	73.5m
Distance cylinders for the stereo-camera system - **Upper limit**	283m	290m
Distance cylinder radius	372.5m	502m
Distance cylinders for the radar system - **Lower limit**	70m	70m
Distance cylinders for the radar system - **Upper limit**	290m	290m

2.1 The stereo-camera system designed by IdentiFlight

The ‘mobile IdentiFlight’ (IDF) stereo-camera system uses 8 wide-angle cameras on a 10m mast to monitor 3D airspace for protected bird species. Objects are filtered, identified and classified using a high-resolution stereo camera, with flight paths monitored at a frequency of 10 Hz and documented with 4D positional accuracy. The system is calibrated several times a day using standard colour calibration plates (KNE, 2021). An Artificial Intelligence (AI) image classifier integrated into the IDF system can detect kites and other birds of prey in combination with photo-optical systems using several different methods of image recognition and classification. If a protected species is detected, the system can trigger the shut-down of one or more wind turbines. This system includes object detection and various machine-learning algorithms based on correctly labelled training data. These AI algorithms can be trained to recognize specific bird species based on unique physical characteristics such as size, shape, colour and markings.

2.2 The radar system designed by BirdScan

The BirdScan Radar System (BSR, Figure 4 right) is used to monitor bird-like targets in real time. It is equipped with an RGB camera, weather sensor and data processing software to classify and validate targets using 4 radar antennae for 360° surveillance. The radar uses Frequency Modulated Continuous Radar Waves to determine the speed of targets. The radar signal monitors all reflections of objects in the airspace and, if a protected species is detected, the system can trigger one or more wind turbines to shut down. To detect and classify objects, the system uses flight behaviour and radar reflectivity, supported by a machine learning algorithm. The radar antennae track and classify all targets in the 3D airspace being monitored. Common CPU interfaces can be used to trigger a shutdown command for one or more WTs if the system detects a protected species.

2.3 Control measurements and bird detection

The detection rate of both ACSs was controlled by experienced regional birdwatchers using an independent, standard bird-monitoring method based on the visual tracking of bird flight paths, measured by a Laser Range Finder system (LRF) (Figure 5). During more than 400 monitoring hours on 56 days in 2022, two birders using handheld LRF systems monitored more than 800 individual 3D bird tracks, providing statistical validation of the detection, correct classification and tracking in the 3D airspace around the simulated WTs. The birdwatchers monitored 426 Red Kite and 343 White-tailed Eagle tracks with the LRF systems at both research sites (Figure 6). A total of 278 LRF tracks of the Red Kite and 212 of the White-tailed Eagle were later used to verify and spatially control the data monitored by the IDF and/or the BSR system in a 3D GIS application. Most of the birds tracks monitored by LRF were also visible to both the camera and the radar systems.

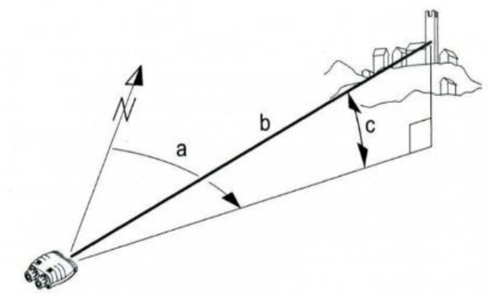

Figure 5: Laser Range Finder Principle (LRF manuals, 2019, and BirdScan, 2020)

Figure 6: Position of a birdwatcher using Laser Range Finder system in August 2022 (photo Mund, 2022)

3 Results and analysis of the IDF stereo-camera system

A total of 62,400 tracks with more than 1.3 million survey points were recorded by the IDF stereo-camera system during the survey period from 15 May to 28 November 2022. About 60% of the trails were recorded in the complex landscape area (site 2), and about 40% in the open farmland area (site 1) (Figure 3). A dense point cloud of more than 1.35 million points (Figure 7) was obtained by plotting all IDF bird detections at the research sites in a two-dimensional graph. The x-axis corresponds to the direction of the sky (= azimuth angle to the north), and the y-axis to the altitude of a bird above ground (= pitch gradient angle).

The orange line at the bottom is the result of topographic masking of areas invisible to the IDF system caused by landscape objects such as hedges or trees. There is hardly any difference between the two observation sites in terms of masking at lower latitudes, while the point cloud of site 1 is clearly less dense than that for site 2 in the NW and ESE directions. This is due to linear landscape elements on the horizon and the exposed location of the IDF on a hill at location 2. The vertical distribution shows that the majority of data points (>65%) were recorded below 15° inclination. Points closer to the ground are unevenly distributed in the direction of the sky. Bird observations with larger elevation angles, >30° above the ground, are more evenly distributed (Figure 7).

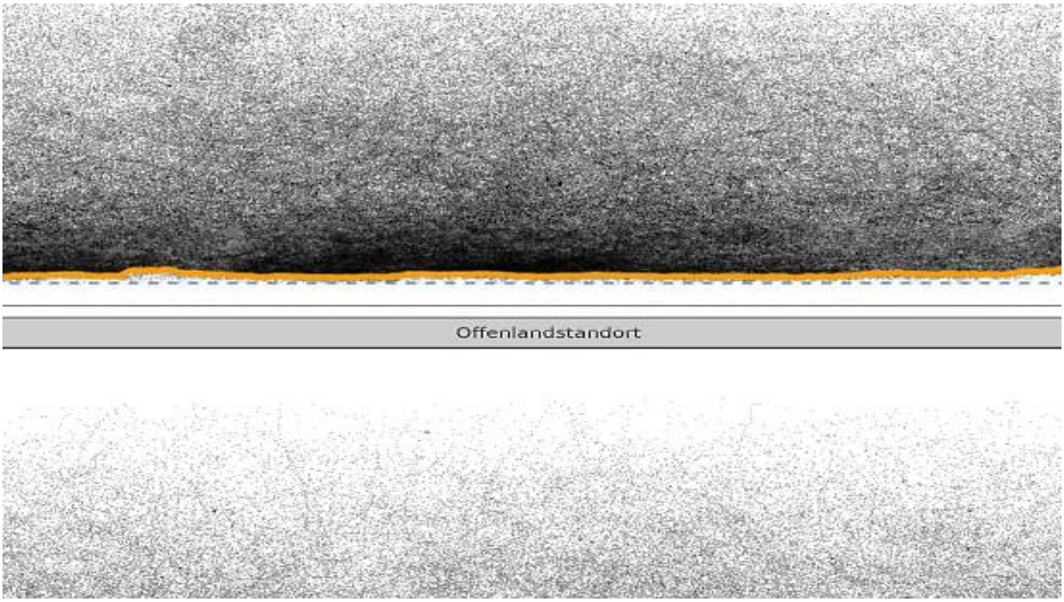

Figure 7: Masking of the IDF scan area in the vertical cylinder plot; graphic based on 1.35 million scan points from the 2022 observation period (adapted from ARSU, Oekofor 2022, unpublished)

Spatial reorganization of segmented tracks resulted in a total of 694 validated segmented Red Kite tracks and around 1,900 validated segmented tracks of the White-tailed Eagle. All individual point scans and tracks were saved in a geospatial database. Using an adapted spatial-temporal point-to-line function in QGIS, we grouped all point data based on the sequenced time stamps to realistic tracks and then interpolated them to individual 3D bird tracks. At study site 1, this resulted in 766 realistic tracks. 401 of these were later compared to and validated using identically time-stamped LRF tracks. The IDF stereo-camera system recorded 374 identified and correctly classified tracks. This corresponds to a classification accuracy of 90.5% for the Red Kite and 96% for the White-tailed Eagle at the open agricultural site (Table 3).

Table 3: Detection rate by species at site 1 (flat open agricultural landscape), validated by LRF reference data

Bird species	LRF tracks in total	validated LRF tracks	invisible IDF tracks	IDF bird species detected	IDF bird species not detected	Other protected bird species
Red Kite	424	201	206	182 (90.5%)	19 (9.5%)	14 tracks
White-tailed Eagle	342	200	124	192 (96%)	9 (4%)	4 tracks

Converting the spatio-temporal point data into lines representing 3D tracks of the birds' movements at survey site 2 resulted in 685 realistic tracks, of which 387 were compared with, and validated by, LRF tracks having the same time stamp. The IDF stereo-camera system recorded 357 identified and correctly classified tracks. This corresponds to an overall classification accuracy of 92.7% for the Red Kite and 91.6% for the White-tailed Eagle in the complex landscape of site 2 (Table 4).

Table 4: Detection rate by species at site 2 (complex undulating landscape), validated by LRF reference data

Bird species	LRF tracks in total	validated LRF tracks	invisible IDF tracks	IDF bird species detected	IDF bird species not detected	Other protected bird species
Red Kite	376	220	146	204 (92.7%)	16 (7.3%)	8 tracks
White-tailed Eagle	309	167	124	153 (91.6%)	14 (8.4%)	7 tracks

An analysis of the horizontal coverage and the maximum vertical detection range for the Red Kite using the IDF stereo-camera system shows a clustering of validated Red Kite points below a vertical range of 200m, and between 200m and 700m horizontal distance from the IDF system.

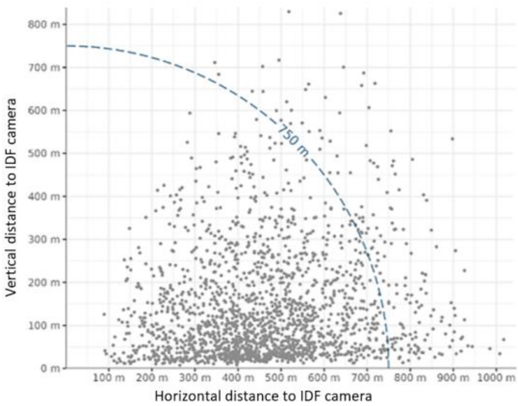

Figure 8: Coverage and detection range of Red Kite using IDF stereo-camera system

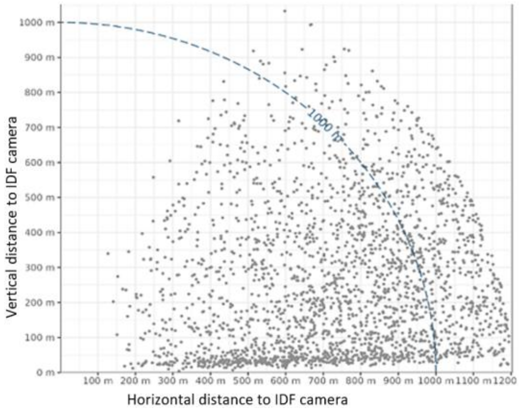

Figure 9: Coverage and detection range of White-tailed Eagle, extract from IDF system

The empirical data collected at both survey points support the required and calibrated 3D range limit of 750m for the detection and classification of the Red Kite (dashed line). Even up to a vertical distance of 850m and a horizontal distance of 1,000m, Red Kites were detected by the IDF camera system (Figure 8).

The analysis of the horizontal coverage and the maximum vertical detection range for the White-tailed Eagle using the IDF stereo-camera system shows a clustering of validated White-tailed Eagle points below 150m vertical range and between 200m and 1,200m horizontal distance from the IDF system. The required and calibrated 1,000m 3D range limit for detection and classification of the species (dashed line) is supported by the empirical data collected at both survey points. The White-tailed Eagle was detected by the IDF camera system even above a vertical distance of 1,000m and above a horizontal distance of 1,200m (Figure 9).

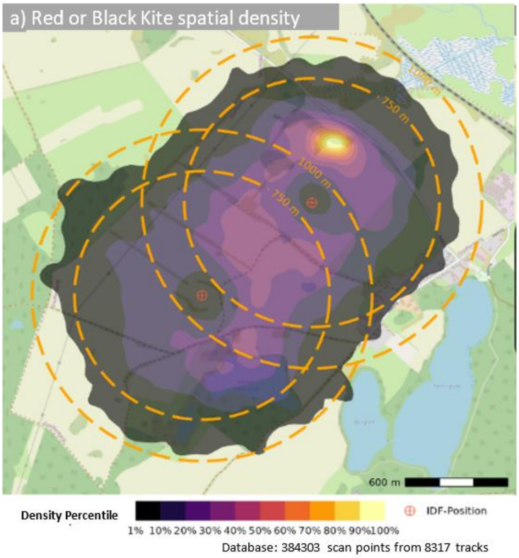

Figure 10: Density of IDF camera scans for Kite movement

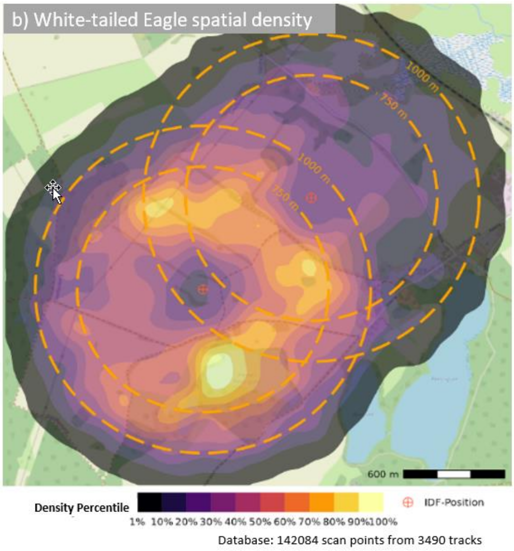

Figure 11: Density of IDF camera scans for White-tailed Eagle

The validated IDF camera scans of protected bird species show different regional density movements in the airspace monitored around the survey sites. The spatial density maps of scattered points were calculated using a kernel function based on individual x,y point patterns; they are presented in percentiles of spatial density per species (Figures 10 and 11). The Red Kite density map shows an obvious spatial concentration in the north-eastern part of the open agricultural area, close to the linear mixed forest groves, where several Red Kite nests were mapped by birdwatchers in 2020. In contrast, the White-tailed Eagle density map shows greater dispersal in the central and southern parts of the study area, where lakes and linear hedgerows dominate. These point data suggest that White-tailed Eagles are less likely to use open agricultural landscapes than kites.

4 Results and analysis of the BirdScan radar system

Throughout the 2022 monitoring period, the BirdScan MS1 R20SS-3D system (BSR) recorded 809 complete and specific Red Kite tracks, and 668 separated White-tailed Eagle tracks. Since the BSR system is capable of detecting up to 512 individual objects at a time, the total database of radar reflection points reaches several million points. Within a moving spatial search window, these points are linked according to their temporal sequence to individual flight tracks of the targeted bird species. Individual bird species detections in single IDF images are used to determine the distance to the virtual WT, while combined bird observation tracks monitor the flight tracks of detected birds. Such bird movement can potentially trigger the shutdown signal.

The BSR system consists of 4 Teledyne FLIR Radar antennae and uses Frequency Modulated Continuous Wave Radar in wavelengths 9.315 to 9.685 GHz. These wavelengths are available for civilian use; they allow the detection of flying birds based on the frequency of their wing beat and their body shape. As radar is an active remote sensing method, the wavelength and pattern of the reflected waves are controlled. This allows for matching with specific, pre-trained object data of birds' movements. Without such additional revised and intensified training of the AI system, the radar monitoring and detection systems are not capable of species-level detection of birds in free airspace.

The BSR bird tracks identified by the LRF at the monitoring sites are distributed differently between the two sites: 329 Red Kite and 309 White-tailed Eagle tracks at site 1 (Figure 14); 490 Red Kite and 359 White-tailed Eagle tracks on the hilltop at site 2 (Figure 15). As the monitoring area of the BSR is much larger than that of the IDF system (up to 5 km in open terrain with no structural obstacles), the number of bird tracks detected and identified is also larger than for the IDF system. Individual flight track segments were spatially linked by merging them into meaningful flight tracks (see Figures 8 and 9). Both figures show examples of bird tracks detected at different times during the monitoring period. In the subsequent interpretation of the data, individual track segments with some spatial or temporal proximity to other tracks, as in the south-eastern corner of the monitoring cylinder, were excluded. The radar data clearly show that the BSR system has the ability to detect the movements of White-tailed Eagles at greater ranges due to the larger size of this species (Figures 12 and 13).

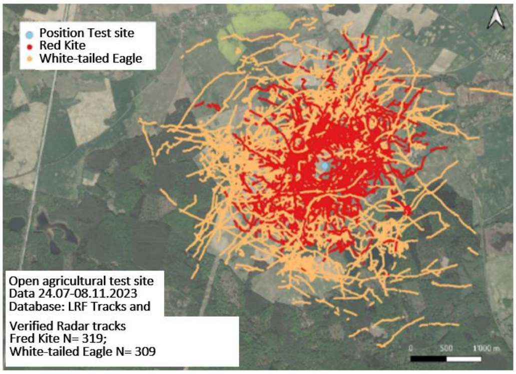

Figure 12: Radar tracks of identified birds at site 1 (open agricultural landscape)

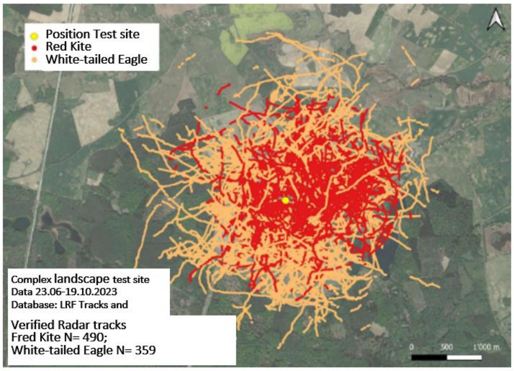

Figure 13: Radar tracks of identified birds at site 2 (complex landscape)

Figures 14 and 15 show individual flight tracks of the two target species and their spatio-temporal relationship to the monitoring and WT exclusion circles. The exclusion circles are at species-specific distances of 502m for the White-tailed Eagle and 372m for the Red Kite. They were calculated using the formulae presented in Section 2, adjusted with empirical values for bird movements published by ARSU 2021. The LRF tracks monitored by the birdwatchers were used to partially verify the tracks of both species presented in Figures 14 and 15.

Figure 14: Example of a Radar and LRF track of a White-tailed Eagle at site 1

Figure 15: Example of a Radar and LRF track of a Red Kite at site 2

The BSR radar detection distance and species detection range were analysed based on the bird tracks detected around the monitoring sites. The radar beam angle was 90° azimuth; a 40° aperture angle was selected for each of the four antennae. Species-specific capture and detection distances varied at both sites: for Red Kite, these were between 150m and 1,900m in the open agricultural landscape, and between 100m and 1,800m in the more complex landscape.

The corresponding results for the White-tailed Eagle were 160m to 2,800m at site 1, and 180m to 2,800m at site 2. The vertical range above ground level for the White-tailed Eagle reaches 900m; for the Red Kite, the maximum is approximately 740m. The slope and undulation of the landscape at a distance of more than 1,000m from each monitoring site (Figures 16 and 17) results in the detection of data points below ground level.

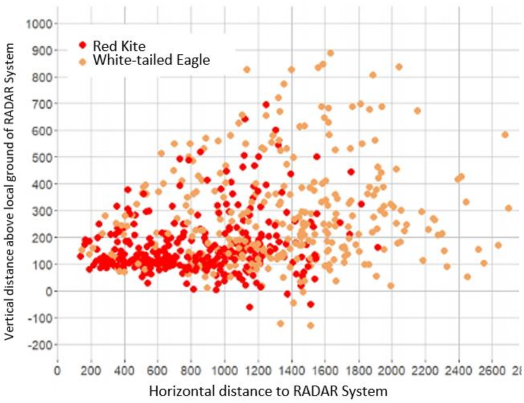

Figure 16: Species-specific detection range of BSR System, site 1

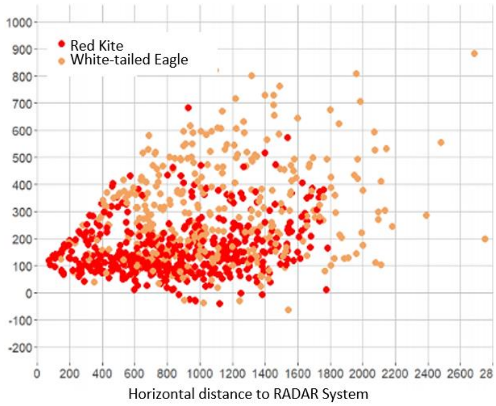

Figure 17: Species-specific detection range of BSR System, site 2

The detection and species-specific classification rates and quality of the BSR system for the Red Kite are shown in Table 5. Overall, there are a high number of identified and correctly classified Red Kite tracks in the inner monitoring circle (monitoring diameter 370m at both sites); the classification accuracy decreases beyond the monitoring circle up to the empirical maximum extent of target bird detection. The empirical data for the White-tailed Eagle show very similar results, although the species detection rate is higher, up to a distance of 2,800m. The BSR species detection rate at both monitoring sites also shows very high detection and classification accuracies within the 700m to 1,400m exclusion cylinder (Tables 6 and 7).

Table 5: Detection and species-specific classification rate for Red Kite at sites 1 and 2

Monitoring site	Horizontal distance	Classification accuracy	Number of tracks
Site 1 open agricultural landscape	0m – 370m	81.5%	9,748
	370m – 740m	77%	25,230
Site 2 complex landscape	0m – 370m	86.2%	7,073
	370m – 740m	77.8%	21,958

Table 6: BSR detection and LRF verified classification rates for both bird species at site 1

Site 1	Red Kite (*Milvus milvus*)		White-tailed Eagle (*Haliaeetus albicilla*)	
Distance range	Flight tracks	BSR detected and LRF verified tracks	Flight tracks	BSR detected and LRF verified tracks
0m – 700m	54	90.7%	27	88.9%
701m – 1,400m	24	70.8%	33	97.0%
1401m – 2,100m	5	40.0%	13	69.2%
2,101m – 2,800m	0	NA	4	50.0%
2,801m – 3,500m	0	NA	1	0%

Table 7: BSR detection and LRF verified classification rates for both bird species at site 2

Site 2	Red Kite (*Milvus milvus*)		White-tailed Eagle (*Haliaeetus albicilla*)	
Distance range	Flight tracks	BSR detected and LRF verified tracks	Flight tracks	BSR detected and LRF verified tracks
0m – 700m	71	91.5%	49	98.0%
701m – 1,400m	52	78.8%	25	84.0%
1401m – 2,100m	8	25.0%	16	56.3%
2,101m – 2,800m	0	NA	4	25.0%
2,801m – 3,500m	0	NA	0	NA

Overall, for both avian target species, the BSR radar system provided a very high detection rate of bird movements in the airspace being monitored. Detection and classification rates of LRF-verified flight tracks were over 90% at distances up to 1,400m to theWT; the classification accuracy was over 70% at distances of more than 1,400m to the WT. Beyond 1400m (outer cylinder), detection and classification rates dropped to 25% for Red Kite and 56% for White-tailed Eagle, which are considered far too low to trigger a correct and verified shutdown signal to the WT.

Finally, the results of the shutdown or retardation signal are important for evaluating the effectiveness of both sensor systems in reducing collisions. In an average of 99.7% of cases, when at least one image of a target species was correctly classified by the IDF, a shutdown signal was generated by the system in the inner distance cylinder (Figures 18 and 19). In 715 bird-monitoring cases, a classified and spatially verified Red Kite position that triggered a shutdown or retardation signal could be assigned to the IDF-induced shutdown signals on the basis of the precise time stamps of the data points. For the White-tailed Eagle, this was possible for 275 flight track positions in the inner protection cylinder of 35 seconds reaction

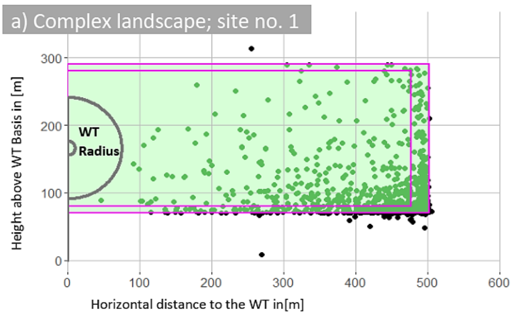

Figure 18: First point of a radar monitored track at which the retardation signal was triggered captured at complex landscape site no 1

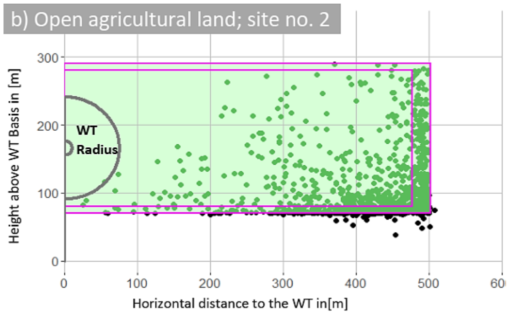

Figure 19: First point of a radar monitored track at which the retardation signal was triggered captured at the open agricultural landscape site no 2

5 Discussion

The empirical results of this paper will be discussed in the light of the following points:

- Technical stability and accuracy of animal monitoring using remote sensing methods
- Representativeness of applied studies and lack of long-term monitoring
- Effectiveness and species accuracy of bird detection
- Policy considerations arising from empirical results.

5.1 Technical stability and accuracy of animal monitoring using remote sensing methods

In many cases in Europe and North America, the implementation of anti-collision systems is specifically tailored to the local bird or bat populations and their migration patterns. This empirical study demonstrates that both ACS systems tested provided safe, permanent and partially redundant technical stability (more than 90% correct bird-species detection) and retardation signal triggered with technical failures or other instabilities below the required <5% level.

Instability of the power supply (generator or battery) was the main cause of the reported failures or system downtime. If these ACSs are installed under normal conditions in wind farms with a permanent connection to a stable power supply, this can be reduced or even eliminated.

The object-detection and image-classification accuracies achieved exceed the required accuracy limit of 90% within the species-specific survey circle – a legal requirement for every ACS installed in the German federal states for the reduction of bird collisions.

Extending the survey period into the late-autumn month of November proved to be challenging for both the BSR and IDF systems in terms of correct species identification and detecting birds at greater distances. During this period, mist and lower seasonal light levels due to the angle of the sun reduced illumination, causing problems with both the BSR and IDF. In November and the winter months, fewer flights of the monitored bird species are to be expected.

5.2 Representativeness of studies of ACSs and lack of long-term monitoring

Many studies on the effectiveness of ACS are recent and conducted over a relatively short period, making it difficult to determine long-term effectiveness (Khosravifard et al. 2017). In addition, some ACS studies are driven by investors in or producers of WT, or lack the necessary representativeness of a scientific study. Scientific impartiality is difficult to achieve in such a politically- and environmentally-driven sector (Bruns et al. 2021). There are also a number of methodological gaps in the current research on the effectiveness of ACSs for wind turbines.

Long-term monitoring is essential to assess the effectiveness of collision-avoidance systems over time and across different typical landscapes. This will help to identify any changes in bird behaviour or population dynamics that may have occurred over several years (Balmori-de la Puente & Balmori, 2023). However, the very high implementation and maintenance costs for research design pose a challenge for the quality, accuracy and durability of ACSs over an extended period. Such barriers require trade-offs in the research design.

The main aim of this study was to test the performance of various high-end ACSs under specific ecological and environmental site conditions without the disturbing presence of working wind turbines. This was essential to monitor the habitat use and behaviour of the target bird species independently. It resulted in the choice of a test site in the economic outer zone of a large biosphere reserve in northeast Germany with a high to very high abundance of many different large bird species, in particular a large population of the target protected species. This decision, with the trade-off of a monitoring period of only one breeding season, allowed the research team to achieve high empirical power. The research design thus omits the variance of generative or seasonal changes in habitat use, which limits the representativeness of this study.

5.3 Effectiveness and species accuracy of bird detection

It is difficult to generalize the results of many recent studies on the effectiveness of avian ACSs, as they have focused on only a few bird species – usually specific protected species. Several studies on the effectiveness of collision-avoidance systems lacked independent control groups. Not surprisingly, the overall number and diversity of migratory, seasonal and resident species captured by both ACS systems and verified by the birdwatchers was high due to the optimal avifaunal-ecological conditions in a protected biosphere reserve. Similar studies are needed that cover a wider range of bird species, and this study can contribute to monitoring a broader range of species present in the region. At a later stage, an analysis of the more diverse avifauna at the site will be published.

The local knowledge and experience of ornithologists is crucial in monitoring and identifying the specific effects of such systems on local avifauna. In this study, birdwatchers recorded any site-specific adaptation or habituation of birds of prey to the two ACS installations for more than 400 monitoring hours. It is important to note that the effectiveness of any ACS – a radar-based or stereo RGB camera – is enhanced by the application of AI image recognition algorithms.

5.4 Political considerations arising from empirical results

In order to achieve the climate protection targets set by the German government, it is essential to promote the environmentally-friendly expansion of wind energy. However, as the KNE notes in a brochure published in 2021 (KNE, 2021), low-conflict areas for onshore wind turbines have become 'scarce'.

Throughout the European Union, wind energy projects in or close to Natura 2000 sites are subject to additional regulatory requirements designed to ensure that WTs do not adversely affect the conservation status of protected species and habitats. Regulations include the implementation of ACSs and the requirement for regular monitoring of bird populations (Kunz & Katzenberger, 2022). Other mandatory measures to protect birds and bats from the negative impacts of wind turbines are also in place in several European countries, including Germany, where failure to implement them can lead to rejection of wind projects or imposition of fines (Bruns et al., 2021). At the same time, the installation of an ACS by a WT developer can demonstrate a commitment to minimizing the negative impacts of wind energy development on wildlife and help to meet the requirements of EU regulatory agencies (Wienhold, 2022).

The option of installing ACSs (or the obligation to do so) at WTs or around wind farms has already been considered in the draft update of the Federal Nature Conservation Act (BNatSchG) in Germany 2023 (§44, 1 BNatSchG) to significantly reduce the risk of fatal accidents to protected birds at WTs.

6 Conclusion

Various anti-collision systems, including physical barriers, acoustic and visual deterrents, and stereo-camera and radar-based systems, have been implemented at many wind farms for more than 10 years. This study showed that two innovative types, stereo camera and radar, have the potential to detect, track and classify certain bird species. The systems can become more effective in reducing bird collisions with WT blades when the close-to 360^0 multi-object scanning capability of all-weather radar systems is combined with the high precision, AI-based image recognition of stereo-camera systems in a new and innovative, hybrid, ACS. The radar system is particularly suitable for special applications (e.g. hotspots in the migration of birds of prey) or for the detection of large numbers of birds over long distances. However, the precision and accuracy of radar-based systems is still inconclusive due to the physical limitation in adaptive modulation of the radar wavelength to specific bird species. Thus, more empirical research in various landscape types and intensified training of radar-specific AI algorithms are needed.

The pre-trained stereo-camera system allows detection, identification, correct classification and monitoring of specific protected bird species with a high level of precision and accuracy, meeting the requirements for WT rotor and blade retardation in terms of the protection of certain species. The potential for further empirical research lies in optimizing machine learning, and in the reduction of the false positive rate, of unnecessary shutdowns, and of the duration of shutdowns. The design and funding of longer empirical monitoring and data sampling periods are strongly recommended.

Acknowledgements

The research project Durchführung von Leistungsnachweisen für Detektionssysteme zur Verminderung von Vogelkollisionen an Windenergieanlagen in Brandenburg was implemented by the HNEE in close cooperation with KNE, ARSU GmbH Ökofor, and the Vogelwarte Sempach in Switzerland. The research is funded by the Ministry of the Economy, Labour and Energy in the state of Brandenburg, Germany (funding number 20020 – 89475). The NGO Kompetenzzentrum Naturschutz und Energiewende gGmbH (KNE) coordinated

communications with stakeholders and civil society, and with the Ministry during the project-implementation phase.

References

Albertani, R.; Johnston, M. L. (2021): A Heterogeneous System for Eagle Detection, Deterrent, and Wildlife Collision Detection for Wind Turbines. Oregon State University, Corvallis, OR, USA. Final Technical Report DE-EE0007885

ARSU GmbH (2021): Wie gut schützt IdentiFlight den Rotmilan (Milvus milvus)? Oldenburg: s.n., 2021. S. 161. Seite 127, 128.

Aschwanden, J.; Liechti, F. (2020): Test of the automatic bird detection system IdentiFlight® on the test field of WindForS in the context of nature conservation research (NatForWINSENT) Schweizerische Vogelwarte Sempach, 2020

Balmori-de la Puente, A.; Balmori, A. (2023): Flight Type and Seasonal Movements Are Important Predictors for Avian Collisions in Wind Farms. Birds 2023, 4, 85-100. https://doi.org/10.3390/birds4010007

BfN; KNE; FA Wind (2020): Technische Systeme zur Minderung von Vogelkollisionen an Windenergieanlagen – Entwicklungsstand und Fragestellungen. BfN-Skript 571.

Bruderer, B.; Boldt, A. (2001): Flight characteristics of birds: I. Radar measurements of speeds. Ibis. 143. 178-204.

Bruns, E.; Schuster, E.; Streiffeler, J. (2021): Anforderungen an technische Überwachungs- und Abschaltsysteme an Windenergieanlagen. In: BfN-Skripten 610. Workshop documentation.

Davy, C.M.; Squires, K.; Zimmerling, J.R. (2021), Estimation of spatiotemporal trends in bat abundance from mortality data collected at wind turbines. Conservation Biology, 35: 227-238. https://doi.org/10.1111/cobi.13554

ENERCON GmbH, Deutschland [Hrsg.] (2020): Technische Beschreibung - Anhalten der Windenergieanlage. 11. 12 2020. Dokument-ID D0630561/2.0-de.

Fachgruppe Rotmilan der Deutschen Ornithologen-Gesellschaft (2022): Stellungnahme Rotmilan-Todesursachen und Gefährdung durch Windenergieanlagen. 21.03.2022.

Georgiev, M.; Zehtindjiev, P. (2022). Real-Time Bird Detection and Collision Risk Control in Wind Farms. Paper presented at WindEurope Electric City 2021, Copenhagen, Denmark.

Gradolewski, D.; Dziak, D.; Martynow, M.; et al. (2021): Comprehensive Bird Preservation at Wind Farms. Sensors. 2021, 21, 267. https://doi.org/ 10.3390/s21010267

Khosravifard, S., Skidmore, A.K., Naimi, B., Venus, V., Muñoz, A.R. and Toxopeus, A.G. (2020), Identifying Birds' Collision Risk with Wind Turbines Using a Multidimensional Utilization Distribution Method. Wildl. Soc. Bull., 44: 191-199. https://doi.org/10.1002/wsb.1056

KNE (2019a): Anforderungen an eine fachlich valide Erprobung von technischen Systemen zur bedarfsgerechten Betriebsregulierung von Windenergieanlagen.

KNE (2019b): Kompetenzzentrum Naturschutz und Energiewende KNE Anfrage Nr. 233 zum Thema Trudelbetrieb und „signifikant erhöhtem Tötungsrisiko“, https://www.naturschutz-energiewende.de/wp-content/uploads/KNE-Antwort_233_OVG_Lueneburg_Trudelbetrieb_seT.pdf

KNE (2020a): Minimizing bird collisions with wind turbines. Can detection systems facilitate an environmentally sound wind energy development? Proceedings of The KKN Conference on May 15–16, 2019 in Kassel.

KNE (2020b): Synopse – Detektionssysteme zur ereignisbezogenen Abschaltung von Windenergieanlagen zum Schutz von tagaktiven Brutvögeln.

KNE (2021): Anforderungen an Antikollisionssysteme zum Schutz von Vögeln an Windenergieanlagen Checkliste für eine qualifi. Entscheidung über die Anwendbarkeit von Antikollisionssystemen. 14 S

KNE (2022): Individuen- und Populationsschutz beim Ausbau der Windenergie an Land – Eine Einführung in die Thematik. 10 S.

Krüger, O.; Grünkorn, T.; Struwe-Juhl, B. (2010): The return of the White-tailed Eagle (Haliaeetus albicilla) to northern Germany: modelling the past to predict the future. In: Biological Conservation. 143 (3)

Lag Vsw (2015): Abstandsempfehlungen für Windenergieanlagen zu bedeutsamen Vogellebensräumen sowie Brutplätzen ausgewählter Vogelarten (Stand April 2015). Berichte zum Vogelschutz 51:15–42

Langgemach, T.; Dürr, T. (2021): Informationen über Einflüsse der Windenergienutzung auf Vögel. In: Landesamt für Umwelt Brandenburg, Staatl. Vogelschutzwarte. https://lfu.brandenburg.de/sixcms/media.php/9/Dokumentation-Voegel-Windkraft.pdf

LRF manuals 2019, and BirdScan, 2020

Masden, E., A.; Haydon, D. T. ; Fox, A.D. et al. (2009): Barriers to movement: impacts of wind farms on migrating birds, *ICES Journal of Marine Science*, Volume 66, Issue 4, May 2009, Pages 746–753, https://doi.org/10.1093/icesjms/fsp031

NABU (2016): Hintergrund | - Faktencheck Rotmilan Und Windenergie. Rotmilan und Windenergie – ein Faktencheck mit Stellungnahmen zu Dokumenten aus der Windenergiebranche. Lars Lachmann, Naturschutzbund Deutschland (NABU) e.V. Charitéstraße 3, 10117 Berlin, www.NABU.de.

NABU (2022): Rotmilan und Windenergieanlagen. Antwort auf den ZDF-Bericht „Rotmilan gegen Windkraftanlagen – Das Märchen vom bedrohten Greifvogel" (https://blogs.nabu.de/rotmilan/). https://blogs.nabu.de/rotmilan/ (25.02.2022).

OVG Lüneburg. (2019). Niedersächsisches Landesjustizportal. 29. 04 2019. Einstweilige Maßnahmen zur Sicherung eines Rechts auf Unterlassung zum Betrieb von bereits errichteten Windenergieanlagen. 12 ME 188/18.

Kunz, F. & Katzenberger, J, Rotmilan Group of the German Ornithological Society, (2022): Ergebnisse der Rotmilan-Schlafplatzzählung 2022, online: https://www.dda-web.de/downloads/publications/rotmilan_spz_ergebnisse_2022.pdf

Wienhold, N. (2022): Rotmilane erkennen Gefahrenbereich des Rotors. In: erneuerbare Energien 03/2022.